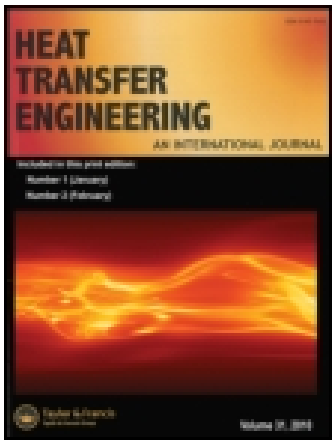

Heat Transfer Engineering
Publication details, including instructions for authors and subscription information:
http://www.tandfonline.com/loi/uhte20

Effects of High-Order Slip/Jump, Thermal Creep, and Variable Thermophysical Properties on Natural Convection in Microchannels With Constant Wall Heat Fluxes

Behnam Rahimi[a] & Hamid Niazmand[a]
[a] Mechanical Engineering Department, Ferdowsi University of Mashhad, Mashhad, Iran
Accepted author version posted online: 04 Mar 2014.Published online: 29 Apr 2014.

To cite this article: Behnam Rahimi & Hamid Niazmand (2014) Effects of High-Order Slip/Jump, Thermal Creep, and Variable Thermophysical Properties on Natural Convection in Microchannels With Constant Wall Heat Fluxes, Heat Transfer Engineering, 35:18, 1528-1538, DOI: 10.1080/01457632.2014.897567

To link to this article: http://dx.doi.org/10.1080/01457632.2014.897567

Heat Transfer Engineering, 35:1528–1538, 2014

ISSN: 0145-7632 print / 1521-0537 online
DOI: 10.1080/01457632.2014.897567

Taylor & Francis
Taylor & Francis Group

Effects of High-Order Slip/Jump, Thermal Creep, and Variable Thermophysical Properties on Natural Convection in Microchannels With Constant Wall Heat Fluxes

BEHNAM RAHIMI and HAMID NIAZMAND

Mechanical Engineering Department, Ferdowsi University of Mashhad, Mashhad, Iran

Natural convection gaseous slip flows in open-ended vertical parallel-plate microchannels with symmetric wall heat fluxes are numerically investigated. A second-order model, including thermal creep effects, is considered for velocity slip and temperature jump boundary conditions with variable thermophysical properties. Simulations are performed for wide range of Rayleigh numbers from 5×10^{-6} to 5×10^{-3} in the continuum to slip flow regime. The developing and fully developed solutions are examined by solving the Navier–Stokes and energy equations using a control volume technique. It is found that the second-order effects reduce the temperature jump and the slip velocity, whereas thermal creep strongly increases the slip velocity in both developing and fully developed regions. Moreover, the rarefaction effects increase the flow and heat transfer rates considerably, while decreasing the maximum gas temperature and friction coefficient as compared to the continuum limit. It was also shown that the axial temperature variations of the gas layer adjacent to the wall in the modeling of the thermal creep are of paramount importance and neglecting these variations, which is common in literature, leads to unphysical velocity and temperature distributions.

INTRODUCTION

Gaseous flow in microscale devices has been in the vanguard of research activities and has received great deal of attention in recent years, due to the rapid growth of applications in micrototal analysis systems and microelectromechanical systems (MEMS). These applications have raised interest in understanding the physical aspects of fluid flow and convective heat transfer in both forced and natural forms through micrometer-sized channels, known as microchannels.

Natural convection has been applied to many engineering fields, such as ventilation cooling of electronics devices [1] and thermal design of MEMS devices [2], because of its reliability and low costs of manufacturing and maintaining [3]. Natural convection is also an area of interest for enhancement of heat and mass transfers in biochemical systems and in micro-fuel-cell devices [4]. Therefore, the study of the rarefaction effects on natural convection may be applicable to designs of these devices in microscale.

Gas flows in microchannels are associated with some degree of rarefaction effects even in a normal pressure environment; hence the continuum hypothesis may not be appropriate for the microchannel flows. The extent of deviation from the continuum is well characterized by the Knudsen number, defined as the ratio of the mean free path to the characteristic length of the physical system [5]. Flows with Knudsen numbers ranging from 0.001 to 0.1 are in the slip flow regime, where slight rarefaction effects are present. It is well established that for the slip flow regime, the Navier–Stokes equations can still be used in conjunction with the modified boundary conditions that are velocity slip and temperature jump conditions [6–8].

The thermal creep phenomenon is also a rarefaction effect related to the streamwise temperature gradient of the fluid. There is a possibility to generate a flow by the tangential temperature gradients along the microchannel walls, which move the fluid in the direction of increasing temperature. Therefore, in such flows the momentum and energy equations are coupled through thermal creep effects.

Address correspondence to Professor Hamid Niazmand, Mechanical Engineering Department, Ferdowsi University of Mashhad, Mashhad, Iran. E-mail: niazmand@um.ac.ir

In contrast to the forced convection gas flows in microsystems that have received proper attention in the literature, very limited studies are available with regard to the natural convection in vertical microchannels. One of the early studies was presented by Chen and Weng in 2005 [9]. They have performed an analytical study on the fully developed natural convection in a vertical parallel-plate microchannel with asymmetric wall temperature. It was shown that the rarefaction effects enhance the flow rate, while reducing the heat transfer rate. Implicit finite-difference simulation of the developing natural convection was presented by Haddad et al. [10] for an isothermally heated microchannel filled with porous media. Biswal et al. [11] investigated the flow and heat transfer characteristics in the developing region of free convection flow in an isothermal vertical microchannel using the semi-implicit method for pressure-linked equations (SIMPLE). They considered the first-order velocity and temperature jump conditions. Also, they illustrated the importance of entrance region and microscale effects on the enhancement of heat transfer rate. Chen and Weng [12] used a marching implicit procedure for modeling the developing natural convection in an open-ended vertical parallel-plate microchannel with asymmetric wall temperature distributions. Chakraborty et al. [13] conducted a boundary-layer integral analysis to evaluate the implications of the developing region in vertical microchannels with constant wall temperatures. Avci and Aydin [14] analytically studied the fully developed mixed convective gas flows in a vertical microchannel with asymmetric constant wall temperatures. The same authors further extended their study to the case of microchannels with constant wall heat fluxes [15], where it was found that the Nusselt number increases slightly as $\mathrm{Gr/Re} = (g\beta q D^4/k(\mu/\rho)^2)/(\rho v_{ave} D/\mu)$ increases. The influence of variable thermophysical properties on the natural convection in a vertical microchannel with asymmetric wall temperatures was investigated by Weng and Chen [16].

Weng and Chen [17] emphasized the importance of thermal creep in the natural convective gas microflows with constant wall heat fluxes using an analytical solution for a fully developed region. However, the adopted reference values for the wall heat flux and the channel width lead to nonphysical high temperature distributions within the channel, which is also inconsistent with the constant thermophysical properties assumption. Weng and Chen [18] investigated the natural convection in an open-ended vertical annular isothermally heated microchannel based on the analytical solution of fully developed region. Recently, Buonomo and Manca [19] numerically investigated the steady-state developing natural convection in a vertical parallel-plate channel with wall spacing of 10 mm and asymmetric uniform heat fluxes at reduced pressure environment. They used the first-order model for slip and jump boundary conditions without considering the thermal creep and variable thermophysical properties effects.

The preceding literature survey indicates the shortage of information regarding the effects of second-order boundary conditions, thermal creep, and variable thermophysical properties on the natural convection in microchannels with wall heat fluxes. As a first study on this topic, a comprehensive computational study has been performed in the entrance and fully developed regions in vertical microchannels at constant wall heat flux conditions. Thermal creep effects along with the second-order slip/jump boundary conditions are considered for different values of Rayleigh and Knudsen numbers. In particular, the temperature-dependent thermophysical properties, which are important in this type of flow, are taken into consideration. Furthermore, some comments have been made on the common assumptions regarding the thermal creep modeling [12, 17] and their inconsistencies with the physics of the problem.

PROBLEM FORMULATION

Consider a vertical parallel plate microchannel and Cartesian coordinates x and y, as shown in Figure 1. The channel height (H) is much larger than the width (D) to ensure the fully developed flow conditions at the channel exit. Both ends of the channel are open to the ambient air with temperature T_0. The microchannel walls are subjected to uniform and constant heat fluxes. Natural convective flows in microchannels are associated with low Reynolds number due to the low velocities and small length scale. For rarefied flows the Mach number is directly related to the Reynolds and Knudsen numbers [6]. Therefore, the compressibility effects for these typically very low Mach number flows are negligible [9, 20]. Considering the Boussinesq approximation, the governing equations for two dimensional, steady, laminar, and incompressible flows with temperature-dependent thermophysical properties [21] are as follows:

$$\frac{\partial u}{\partial x} + \frac{\partial v}{\partial y} = 0 \tag{1}$$

$$\rho\left(u\frac{\partial u}{\partial x} + v\frac{\partial u}{\partial y}\right) = -\frac{\partial p}{\partial x} + \frac{\partial}{\partial x}\left(\mu\frac{\partial u}{\partial x}\right) + \frac{\partial}{\partial y}\left(\mu\frac{\partial u}{\partial y}\right) \tag{2}$$

$$\rho\left(u\frac{\partial v}{\partial x} + v\frac{\partial v}{\partial y}\right) = -\frac{\partial p}{\partial y} + \frac{\partial}{\partial x}\left(\mu\frac{\partial v}{\partial x}\right) + \frac{\partial}{\partial y}\left(\mu\frac{\partial v}{\partial y}\right) + \rho g\beta\,(T - T_0) \tag{3}$$

$$u\frac{\partial\left(\rho c_p T\right)}{\partial x} + v\frac{\partial\left(\rho c_p T\right)}{\partial y} = \frac{\partial}{\partial x}\left(k\frac{\partial T}{\partial x}\right) + \frac{\partial}{\partial y}\left(k\frac{\partial T}{\partial y}\right) + \mu\left[2\left\{\left(\frac{\partial u}{\partial x}\right)^2 + \left(\frac{\partial v}{\partial y}\right)^2\right\} + \left(\frac{\partial u}{\partial y} + \frac{\partial v}{\partial x}\right)^2\right] \tag{4}$$

Where β is the volumetric thermal expansion coefficient, μ is the dynamic viscosity, c_p is the specific heat at constant pressure,

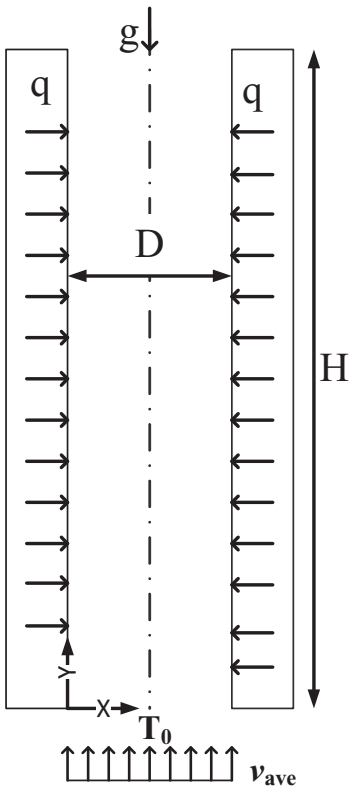

Figure 1 Flow geometry and the coordinates system.

and k is thermal conductivity. The viscous dissipation term is also included in the energy equation.

Based on the gas kinetic theory, the second-order slip model suggested by Karniadakis and Beskok [7] relates the slip velocity to the local velocity gradients at the wall as:

$$v_s = \frac{2-\sigma_v}{\sigma_v}\left[\mathrm{KnD}\left(\frac{\partial v}{\partial x}\right)_g + \frac{(\mathrm{KnD})^2}{2}\left(\frac{\partial^2 v}{\partial x^2}\right)_g\right] + \frac{3}{4}\frac{\mu}{\rho T_g}\frac{\partial T}{\partial y} \tag{5}$$

In this equation, the terms in the bracket are the slip velocity due to the shear stress at the wall, while the last term is the thermal creep velocity due to a temperature gradient tangential to the wall. Thermal creep implies that the tangential temperature gradient of the gas layer adjacent to the wall can introduce a fluid flow in the absence of any other deriving forces in the direction of cold to hot. This term is especially important in the entrance region, where the streamwise temperature gradients of the gas layer in the vicinity of the wall are more pronounced. For the molecules that are not thermally accommodated with the wall, there is a temperature discontinuity and the kinetic theory expression for the second-order temperature jump boundary condition is [7]:

$$T_s - T_w = \frac{2-\sigma_t}{\sigma_t}\frac{2\gamma}{\gamma+1}\frac{1}{\mathrm{Pr}} \times \left[\mathrm{KnD}\left(\frac{\partial T}{\partial x}\right)_g + \frac{(\mathrm{KnD})^2}{2}\left(\frac{\partial^2 T}{\partial x^2}\right)_g\right] \tag{6}$$

where T_s is the temperature of the gas layer adjacent to the wall, T_w is the wall temperature, and γ is the specific heat ratio. Also, σ_v and σ_t are the tangential momentum and energy accommodation coefficients, which are determined experimentally. However, their values for most engineering applications are approximately around 1, which is also the adopted value in the present study. The molecular mean free path, λ, is related to the gas temperature and viscosity. Therefore, in variable-property simulations, the Knudsen number and mean free path are related to the temperature of the gas as [22]:

$$\lambda = \lambda_0\left(\frac{T}{T_0}\right)^{0.5+n_\mu} \tag{7}$$

where n_μ is the viscosity index, and for air as the working fluid, it is assumed to be equal to 0.712 [23]. Thus, the temperature-dependent Knudsen number is:

$$\mathrm{Kn} = \frac{\lambda}{D} = \frac{\lambda_0}{D}\left(\frac{T}{T_0}\right)^{1.212} = \mathrm{Kn}_0\left(\frac{T}{T_0}\right)^{1.212} \tag{8}$$

It is worth mentioning that in the already-mentioned slip velocity and temperature jump formulations (Eqs. 5 and 6) the mixed derivatives, which are considered in more complicated models as indicated in Weng and Chen [24], are neglected. The effects of the mixed derivatives, $\partial^2 u/\partial x\partial y$ and $\partial^2 T/\partial x\partial y$, on the slip/jump values in the present problem have been studied and were found to be negligible. For instance, from the Maxwell–Burnett slip law [25] the maximum contributions of the velocity and temperature mixed derivatives to the slip velocity are about 1%. Therefore, the Karniadakis–Beskok slip/jump boundary conditions [7], which neglect the mixed derivatives, are considered to be valid boundary conditions for the present problem.

For the inlet boundary conditions, $u = 0$, $v = v_{ave}$, and $T = T_0$ are assumed. It should be noted that v_{ave} is updated according to the exit mass flow rate at each iteration. For all flow variables, zero gradients at the outlet are applied except for the temperature gradient, which is constant, consistent with the fixed applied heat fluxes. At walls, slip velocity and temperature jump conditions according to Eqs. (5) and (6) are employed. Corresponding to the constant wall heat flux condition, the normal temperature gradient is given and equal to:

$$\left(\frac{\partial T}{\partial x}\right)_g = \frac{q}{k} \tag{9}$$

where q is the imposed heat flux. The local Nusselt number is evaluated according to:

$$\mathrm{Nu} = \frac{qD}{(T_w - T_0)\,k_0} \tag{10}$$

The local friction coefficient is defined as [17]

$$\Gamma = \frac{D}{v_c}\left(\frac{\partial v}{\partial x}\right)_g \tag{11}$$

where v_c is the characteristic velocity and is given by [26]

$$v_c = \frac{\rho_0 g \beta q D^3}{\mu_0 k_0} \tag{12}$$

The nondimensional volume flow rate, which is commonly used as a velocity normalization parameter, can be written as

$$M = \int_0^1 \frac{v}{v_c} dx' \tag{13}$$

where dimensionless channel width is $x' = \frac{x}{D}$.

NUMERICAL MODELING AND VALIDATIONS

The governing equations are solved using a finite-volume approach. The convective terms are discretized using the hybrid scheme, while for diffusive terms central differencing is employed. Coupling between the velocity and pressure is made with the SIMPLE algorithm [27]. The resultant system of discretized linear algebraic equations is solved with an ADI scheme. Extensive computations have been performed to identify the number of grid points that produces reasonably grid independent results. It was found that the solution is relatively sensitive to the number of grid points in the axial and cross-sectional directions. The quantities examined for this matter are the maximum temperature and volume flow rate. Table 1 presents the grid resolution studies for volume flow rate, M, and the maximum of nondimensional temperature, $\theta = \frac{T-T_0}{\frac{qD}{k}}$. Therefore, a system of 150 × 800 grid points is used in the cross-sectional and axial directions, respectively, to discretize the domain with aspect ratio of 30. The convergence criterion for the iterative procedure are the overall energy balance residual less than 1% and $|(\Psi - \Psi_{old})/\Psi_{max}| \leq 10^{-5}$, where Ψ represents the flow variables and Ψ_{max} is the maximum value of the variable in the entire domain.

The numerical scheme has been validated by comparing the fully developed velocity and temperature profiles with the analytical solutions of Weng and Chen [17] as shown in Figures 2 and 3, respectively. In the following, for temperature profiles

Table 1 Grid resolution effects on the maximum temperature and the volume flow rate

Grid	θ_{max}	M
300 × 1600	1498.15	74.05
150 × 1600	1498.95	74.58
300 × 800	1497.50	74.69
150 × 800	1501.29	74.37
75 × 800	1434.87	71.31
150 × 400	1566.00	71.22

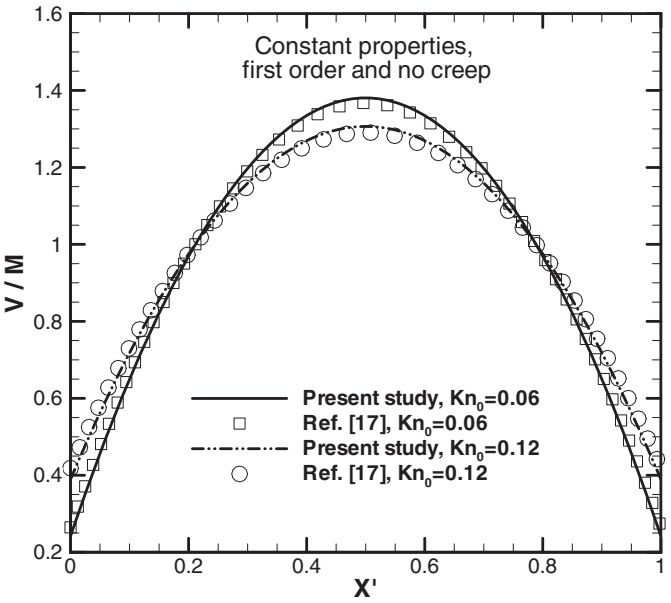

Figure 2 Comparison of the fully developed velocity profiles with those of Weng and Chen [17] at $Ra = 7 \times 10^{-6}$ and $Kn_0 = 0.12$ and 0.06.

the nondimensional profiles of $\theta - \theta_w$ are plotted, which in the fully developed region become invariant in the flow direction. The profiles are obtained for constant thermophysical properties and the first-order slip/jump boundary conditions in absence of the thermal creep effects corresponding to the conditions of reference [17], where good agreements are observed for both Knudsen numbers of 0.06 and 0.12.

For the case of thermal creep, again the fully developed velocity and temperature profiles are compared with the analytical results of Weng and Chen [17] in Figures 4 and 5, respectively.

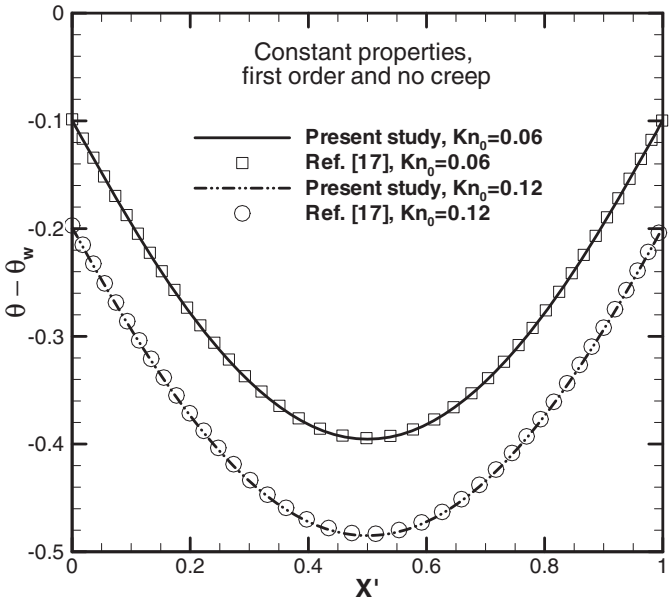

Figure 3 Comparison of the fully developed temperature profiles with those of Weng and Chen [17] at $Ra = 7 \times 10^{-6}$ and $Kn_0 = 0.12$ and 0.06.

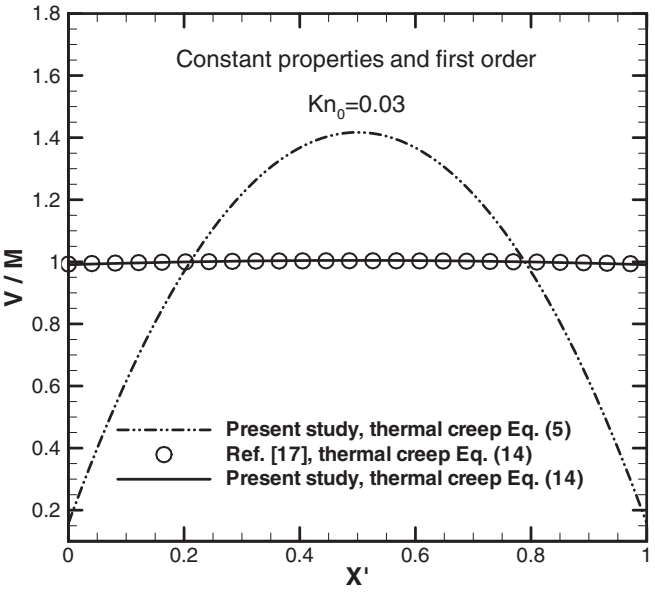

Figure 4 Comparison of the fully developed velocity profiles with those of Weng and Chen [17] in the presence of thermal creep at $Ra = 2.23 \times 10^{-13}$ and $Kn_0 = 0.03$.

Similarly, the constant thermophysical properties and first-order slip/jump boundary conditions are considered for $Kn_0 = 0.03$. It is clear that both profiles agree well with the analytical results of reference [17]. It must be emphasized that for this comparison, the slip velocity equation introduced by reference [17] as

$$v_s = \frac{2-\sigma_v}{\sigma_v}\left[KnD\left(\frac{\partial v}{\partial x}\right)_g\right] + \frac{3}{2\pi}\frac{\gamma-1}{\gamma}\frac{c_{p0}\rho_0}{\mu_0}\lambda^2\frac{\partial T}{\partial y} \quad (14)$$

is employed with reported reference values of $q = 1.09$ W/m^2 and $D = 2.22 \times 10^{-6}$ m. In fact, the preceding equation can be easily obtained from Eq. (5) by neglecting the second-order term and substituting for T_g from the equation of state in the last term related to the thermal creep effects. For the case of constant thermophysical properties, it is a common practice in literature to treat the substituted variables for T_g like density as constants evaluated at the reference inlet temperature [12, 17]. This means that the temperature of the gas layer adjacent to the wall is basically replaced by constant thermophysical properties evaluated at the inlet temperature. Such a treatment can lead to unphysical results since the variations of T_g along the channel are not considered. According to the mentioned reference values, gas temperature variation along the microchannel is about 75,000 K, which is not only nonphysical but also cannot be represented by the constant inlet temperature of about 300 K. If the variation of T_g along the channel is considered as indicated by Eq. (5), even for constant thermophysical properties and the already-mentioned reference values, the velocity and temperature profiles become fairly different from the preceding results as also included in Figures 4 and 5.

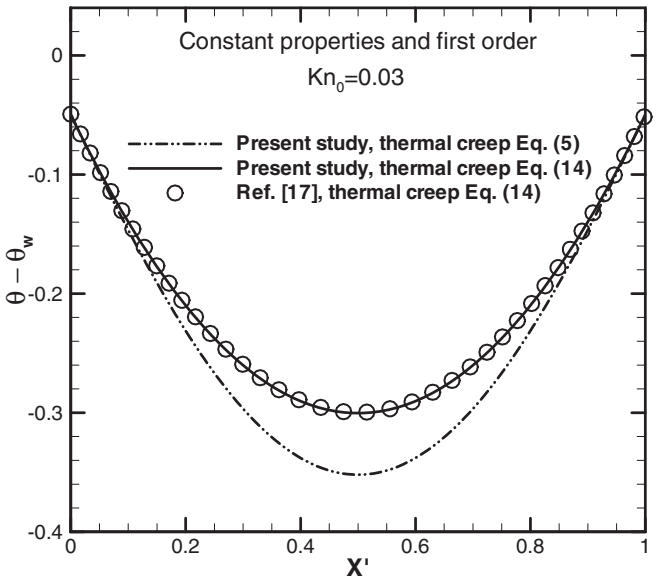

Figure 5 Comparison of the fully developed temperature profiles with those of Weng and Chen [17] in the presence of thermal creep at $Ra = 2.23 \times 10^{-13}$ and $Kn_0 = 0.03$.

RESULTS AND DISCUSSION

The Rayleigh number, defined as $Ra = \frac{\rho_0^2 g c_{p0} \beta q D^4}{k_0^2 \mu_0}$, is a nondimensional parameter that governs the flow and is used in presenting the results here. All referenced thermophysical properties denoted by subscript 0 are evaluated at the inlet air temperature of $T_0 = 273.15$ K. The volumetric thermal expansion coefficient, β, is obtained according to the ideal gas approximation. The applied heat fluxes are in the range of 0.5 to 4 W/m^2 corresponding to the Ra numbers of 5×10^{-6} to 5×10^{-3}. Both the applied heat fluxes and the microchannel widths are adjusted such that the gas temperature distributions remain within a physical range and the resulting driving thermal buoyancy forces are almost similar for all cases at a given Knudsen number. It should be noted that considered values of Raleigh numbers in the present study are much lower than those of Biswal et al. [11] ($100 < Ra < 10^5$), since large values of Ra lead to impractical high temperatures. In all results reported hereafter the thermal creep effects, second-order slip/jump conditions, and variable thermophysical properties are considered unless otherwise stated. Furthermore, it is found that the contribution of the thermal dissipation term to the velocity and temperature fields is not significant, and can be neglected for natural convection microflows.

The developments of velocity profiles in axial and cross sectional directions are presented in Figures 6 and 7, respectively. The velocities are nondimensionalized by the characteristic velocity, $V = \frac{v}{v_c}$ and $U = \frac{u}{v_c}$, and normalized with respect to the nondimensional volume flow rate. Both axial and cross-sectional coordinates are nondimensionalized by the channel width. The inlet Knudsen number of $Kn_0 = 0.06$ is considered for the constant heat flux of 1.8 W/m^2 applied to both walls, corresponding to the Rayleigh number of $Ra = 1.3 \times 10^{-3}$. It

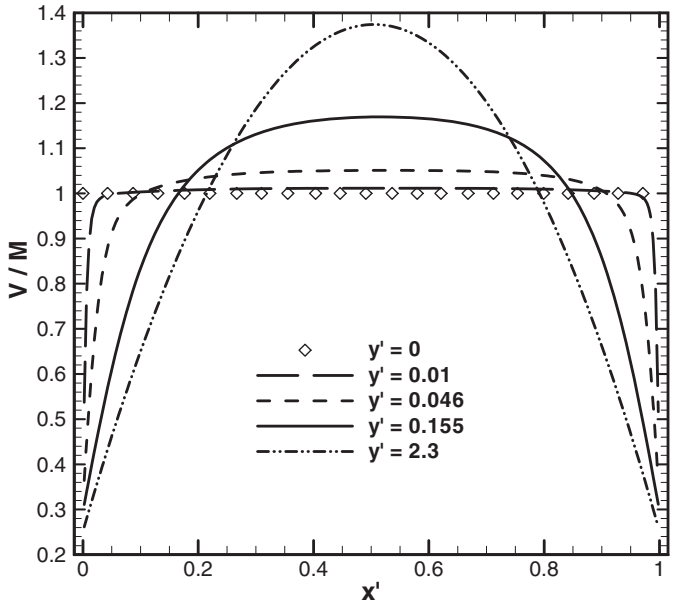

Figure 6 Streamwise velocity profiles at different axial locations for Ra = 1.3×10^{-3} and $Kn_0 = 0.06$.

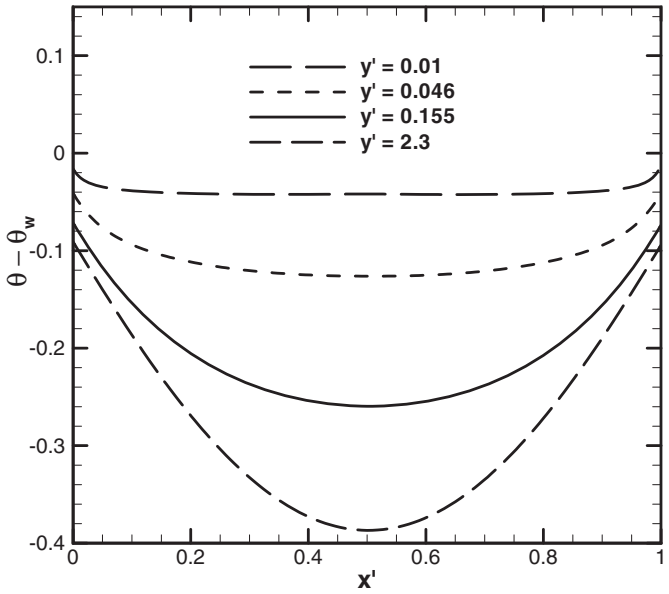

Figure 8 Temperature distributions at different axial locations for Ra = 1.3×10^{-3} and $Kn_0 = 0.06$.

is observed from Figure 6 that the uniform inlet velocity profile transforms into the fully developed profile after passing through considerable variations. The velocity slip is considerable, very close to the inlet, where the uniform inlet velocity profile is dragged by walls leading to large normal velocity gradients. In the fully developed region, the velocity slip approaches a nearly constant value since the velocity profiles and the normal velocity gradients become invariant except for the slight variations in the local Knudsen number due to the variations in temperature. A cross-flow field is formed close to the entrance because of the uniform inlet velocity profile and the dragging effects of the walls as shown in Figure 7. Despite the slip velocity at the wall, the fluid is still slowed down by the wall, leading to strong cross-sectional pressure gradients with regions of high pressure at walls close to the inlet. These localized high-pressure zones at the inlet walls push the fluid toward the channel core, generating the cross-flow velocities. The cross-flow field is only considerable close to the inlet and smears out rather quickly toward the fully developed region, where cross-sectional pressure variations vanish.

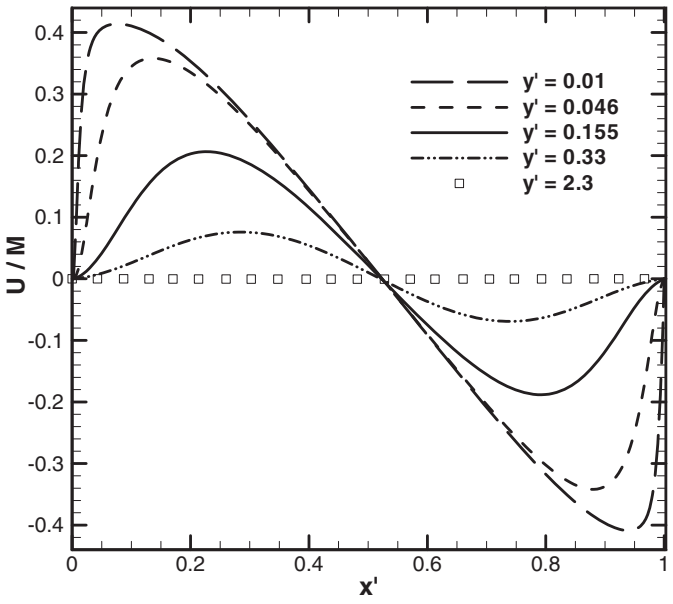

Figure 7 Cross-flow velocity profiles at different axial locations for Ra = 1.3×10^{-3} and $Kn_0 = 0.06$.

In Figure 8 the developments of the temperature profiles along the microchannel are presented for the same flow conditions as those in Figure 6. The temperature differences between the wall and the core regions increase due to the applied heat fluxes at the walls until the heat flux effects reach the core region and the flow becomes thermally fully developed. Note that the values of $\theta - \theta_w$ indicate the temperature jump at the walls, which increase along the channel with a decreasing rate. It should be emphasized that the temperature jump variation along the channel is basically due to the temperature dependence of the Kn number, which varies with temperature according to Eq. (8), and the second-order effect, which is more pronounced at the developing region and decreases the temperature jump.

One of the major effects of rarefaction is the increase in flow rate as can be seen in Figure 9. This figure illustrates the variations of two nondimensional flow rates M and Q as a function of Rayleigh number for different values of the Knudsen numbers. The difference between the volume flow rate Q defined as $Q = \int_0^1 \frac{v}{v_{ns}} dx'$ and M is in the scaling reference velocity, which makes M more suitable for scaling the velocity field, while Q indicates the volume flow rate in a more physical manner. Here the subscript *ns* refers to the no-slip average velocity at

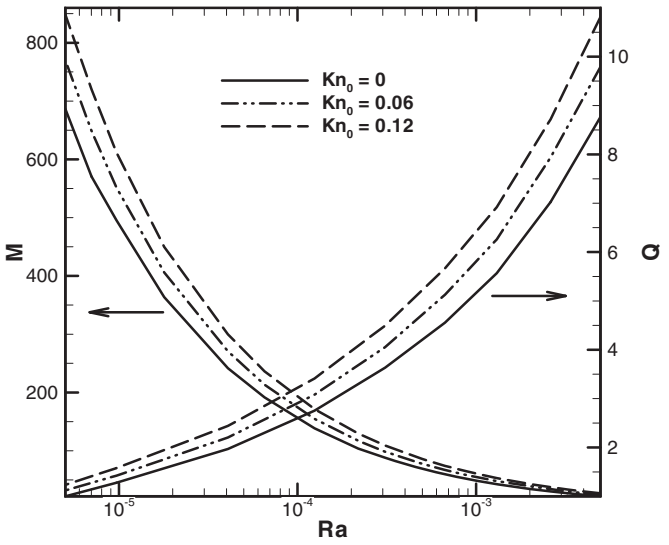

Figure 9 Variations of volume flow rates as a function of the Rayleigh number for different values of Kn_0.

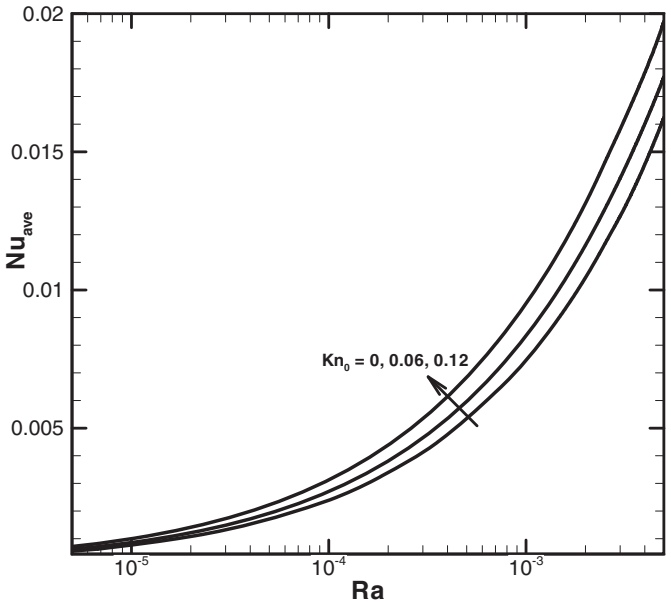

Figure 11 Variations of the averaged heat transfer rates as a function of the Rayleigh number for different values of Kn_0.

$Ra = 5 \times 10^{-6}$ corresponding to the lowest Ra considered in this study. Clearly, the flow rate, Q, increases as the Rayleigh and Knudsen numbers increase, which amounts to about 12% and 24% at $Ra = 1 \times 10^{-3}$ for Knudsen numbers of 0.06 and 0.12, respectively, as compared to the no-slip case.

In Figure 10 the variations of the dimensionless gas temperature in the immediate vicinity of the wall at the end of the microchannel (y = H) are plotted as a function of the Rayleigh number. At this location the gas adjacent to the walls has the maximum temperature. It can be seen that the gas temperature is a decreasing function of Rayleigh and Knudsen numbers, which can be explained by the increase in flow rate with increasing Ra and Kn (Figure 9), which in turn reflects in lowering the flow temperature.

The variations of the averaged heat transfer rates with the Rayleigh number for several values of the Knudsen numbers are plotted in Figure 11. It is obvious that the Nusselt number increases with the Rayleigh number since higher Rayleigh numbers are accompanied by the higher flow rates and the increased entrance lengths, where both effects improve the heat transfer rates. Moreover, these effects are enhanced further in the presence of the rarefaction. For more clarification, the axial

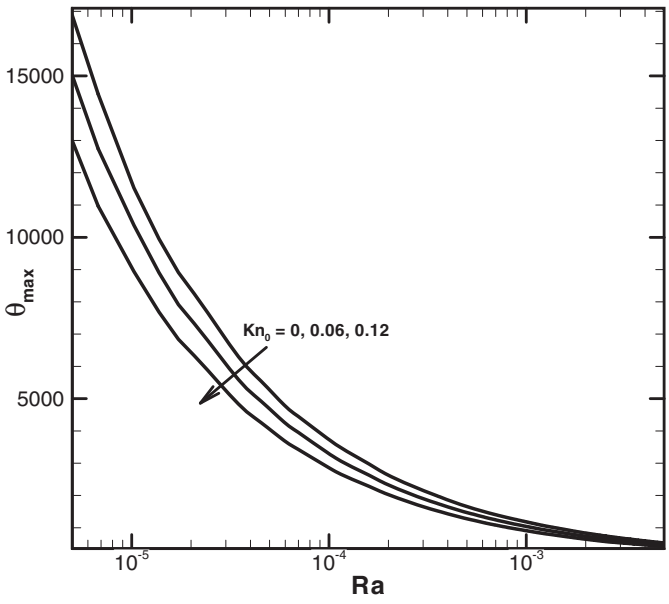

Figure 10 Variations of maximum gas temperature as a function of the Rayleigh number for different values of Kn_0.

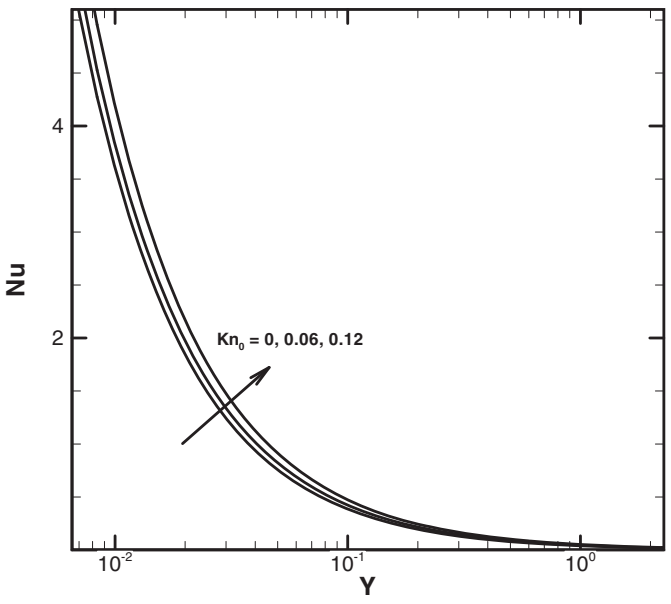

Figure 12 Axial variations of the local Nusselt number at $Ra = 2.6 \times 10^{-3}$ for different values of Kn_0.

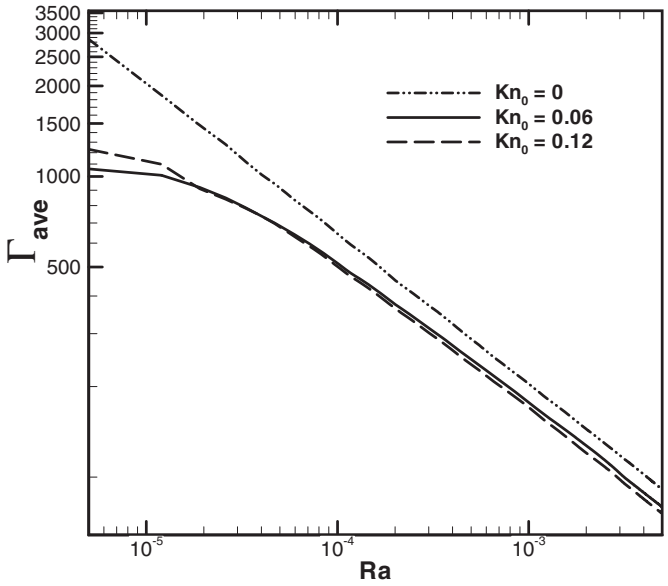

Figure 13 Variations of the averaged friction coefficient as a function of the Rayleigh number for different values of Kn_0.

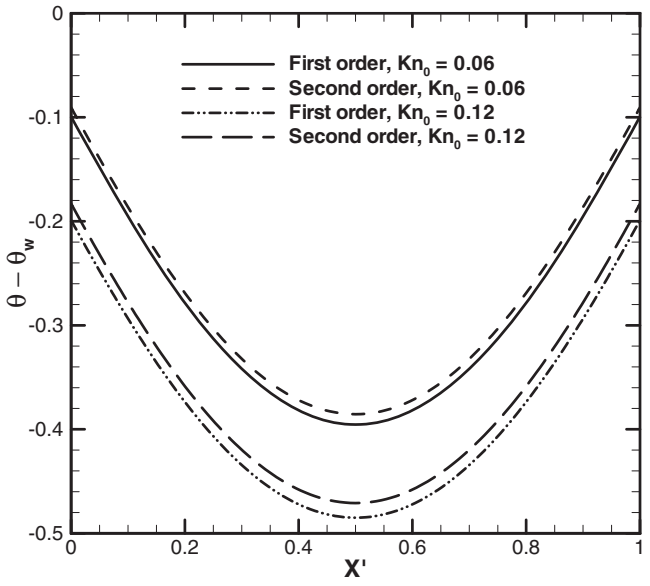

Figure 15 Comparison of the fully developed temperature profiles for first- and second-order boundary conditions at $Ra = 7 \times 10^{-6}$ and $Kn_0 = 0.12$ and 0.06.

variations of the local Nusselt number for a constant Rayleigh number and different values of the Knudsen numbers are plotted in Figure 12. Clearly, slip velocity enhances convection close to the wall, where convective effects are fairly weak, and at the same time increases the entrance length slightly, where the heat transfer rates are higher.

The variations of the averaged friction coefficient as a function of the Rayleigh number for different Knudsen numbers are plotted in Figure 13. It is clear that the averaged friction coefficient decreases with increasing Rayleigh number even in the no-slip limit. To justify this trend one should consider that the flow rate increases with the increase in Ra, as discussed with respect to Figure 9. Considering the fact that the resulting buoyancy force is almost similar for different Ra at a given Knudsen number, the only possible way to increase the flow rate at a constant driving force is the reduction in friction coefficient. The figure also shows that the averaged friction coefficient experiences larger reduction in the presence of the rarefactions effects at lower Rayleigh numbers, and this can be attributed to the thermal creep effects, which are more pronounced at lower Rayleigh numbers. In particular, the contribution of the thermal creep to the slip velocity is more evident at lower Knudsen numbers for low Ra numbers, which can be seen for the case of Kn $= 0.06$ as compared to the case with Kn $= 0.12$. However, at higher Rayleigh numbers the thermal creep contribution to the slip velocity is less dominant as compared to the normal velocity gradients, which are directly related to the Knudsen number, and thus the reduction in average friction coefficient is larger at higher Knudsen numbers.

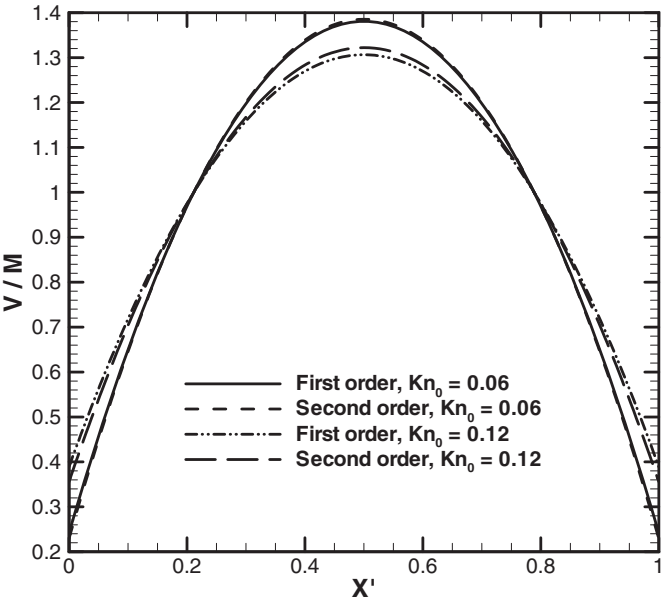

Figure 14 Comparison of the fully developed velocity profiles for first- and second-order boundary conditions at $Ra = 7 \times 10^{-6}$ and $Kn_0 = 0.12$ and 0.06.

The effect of second-order slip/jump boundary conditions on the fully developed velocity and temperature profiles are examined in Figures 14 and 15, respectively. The flow conditions are the same as those in Figure 2. These figures illustrate that the second-order slip/jump effects are more pronounced at higher Knudsen numbers for both profiles. Clearly, second-order effects do not affect the velocity profile, when relatively slight rarefaction effects (Kn ≤ 0.06) are present. It is also interesting to note that the second-order effects reduce the temperature jump and the velocity slip.

Finally, the effects of variable properties and the thermal creep are studied on the fully developed velocity and temperature profiles. In Figure 16 the fully developed velocity profiles for three different cases considering the effects of either thermal creep or variable thermophysical properties or both are plotted

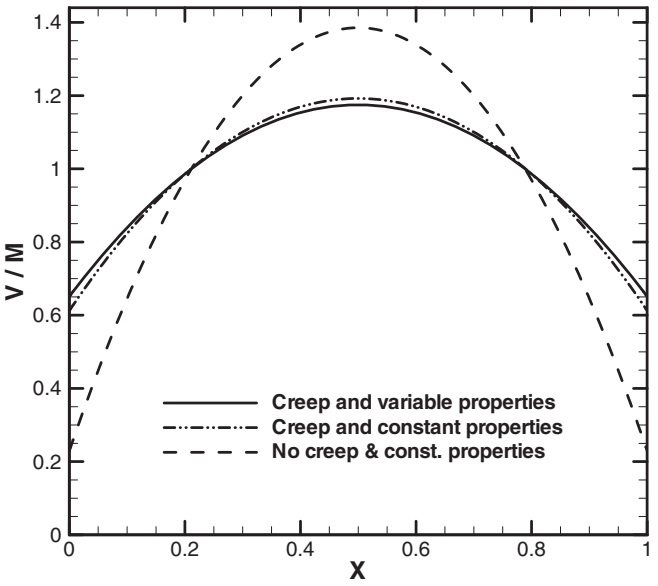

Figure 16 Effects of thermal creep and variable thermophysical properties on the fully developed velocity profiles at $Ra = 7 \times 10^{-6}$ and $Kn_0 = 0.06$.

for $Ra = 7 \times 10^{-6}$ and $Kn_0 = 0.06$. It is clear that the thermal creep strongly affects the velocity profile and leads to considerable increase in slip velocity in the fully developed region. This is in contrast to the constant-temperature wall condition such that thermal creep effects basically vanish in the fully developed region. Furthermore, the increase in the slip velocity for the case of variable properties is mainly because of an increase in the local Knudsen number due to the temperature-dependent properties.

In Figure 17 the fully developed temperature profiles are presented for the same flow conditions as in Figure 16. Figure 17 clearly indicates that the fully developed temperature profiles

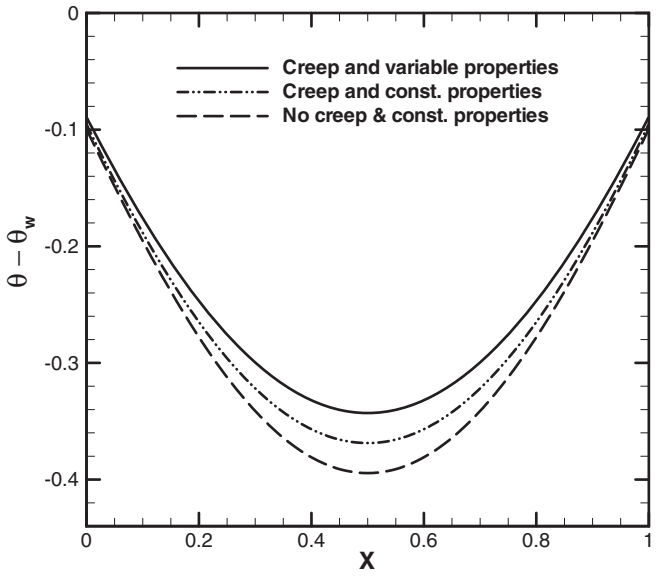

Figure 17 Effects of thermal creep and variable thermophysical properties on the fully developed temperature profiles at $Ra = 7 \times 10^{-6}$ and $Kn_0 = 0.06$.

are affected by both variable properties and thermal creep. Both effects reduce the temperature difference between the wall and the core region. In contrast to the fully developed slip velocity, the temperature jump at the wall is basically not influenced by thermal creep effects.

CONCLUSIONS

A numerical analysis on the developing and developed natural convective gas flows through a symmetrically heated vertical microchannel has been performed. The governing equations subject to the second-order slip/jump boundary conditions including thermal creep with temperature-dependent thermophysical properties are solved using a control volume technique. The numerical scheme validations were established through comparison of the numerical velocity and temperature profiles with their analytical counterparts. Moreover, the second-order, thermal creep, and variable thermophysical properties effects on both developing and fully developed velocity and temperature profiles are examined in detail. The major findings from the present study can be summarized as follows:

1. Substituting for T_g from the equation of state in the modeling of thermal creep (Eq. 14), which is a common practice in literature, leads to unphysical results and the velocity and temperature profiles become fairly different from those obtained by considering the variation of T_g along the microchannel.
2. Temperature jump increases along the channel with a decreasing rate. This is basically due to the temperature dependence of the Kn number and the second-order effects, which are more pronounced at the channel inlet and decrease the temperature jump.
3. An increase in Raleigh number leads to an increase in flow and heat transfer rates, while the maximum gas temperature and friction coefficient decrease. All effects are enhanced in the presence of the rarefaction effects.
4. The reduction in the averaged friction coefficient becomes more prominent at lower Raleigh numbers; however, due to the thermal creep effects this reduction is more pronounced at lower Knudsen numbers.
5. The second-order effects, which are more pronounced in the entrance region and at higher Knudsen numbers, reduce the slip velocity and temperature jump; however, in the fully developed region the velocity and temperature profiles are less influenced by these effects.
6. Thermal creep strongly affects the velocity profile and leads to a considerable increase in the slip velocity in both developing and fully developed regions. This is especially true for the lower Raleigh and Knudsen numbers, where thermal creep contribution to the slip velocity is dominant.

NOMENCLATURE

c_p specific heat at constant pressure, J/kg-K

c_v specific heat at constant volume, J/kg-K
D width of channel, m
g gravitational acceleration, m/s^2
Gr Grashof number
H height of channel, m
k thermal conductivity, W/m-K
Kn Knudsen number, $(\frac{\lambda}{D})$
M dimensionless volume flow rate
Nu local Nusselt number, $(\frac{qD}{(T_w - T_0)k_0})$
p pressure, Pa
Pr Prandtl number, $(\frac{\mu_0 c_{p0}}{k_0})$
q local heat transfer rate(heat flux), W/m^2
Q dimensionless volume flow rate
Ra Rayleigh number based on ambient properties, $(\frac{\rho_0^2 g c_{p0} \beta q D^4}{k_0^2 \mu_0})$
Re Reynolds number
T temperature, K
u velocity components in x direction, m/s
U dimensionless velocity component in x direction, $(\frac{u}{v_c})$
v velocity components in y direction, m/s
v_{ave} average velocity in the y-direction, m/s
v_{ns} no slip velocity at Ra $= 5 \times 10^{-6}$, m/s
V dimensionless velocity component in y direction, $(\frac{v}{v_c})$
x, y rectangular coordinate system
x′, y′ dimensionless rectangular coordinate system, $(x' = \frac{x}{D},\ y' = \frac{y}{H})$

Greek Symbols

β thermal expansion coefficient, K^{-1}
γ specific heat ratio, $(\frac{C_p}{C_v})$
Γ dimensionless local friction coefficient
θ dimensionless temperature, $(\frac{T - T_0}{\frac{qD}{k}})$
λ molecular mean free path, m
μ dynamic viscosity, kg/m-s
ρ density, kg/m^3
σ_t thermal accommodation coefficient
σ_v tangential momentum accommodation coefficient

Subscripts

ave average value in the y-direction
c characteristic value
g gas value near the wall surface
0 ambient values
s wall-slip/jump values
w wall values

REFERENCES

[1] Da Silva, A. K., Lorenzini, G., and Bejan, A., Distribution of Heat Sources in Vertical Open Channels with Natural Convection, *International Journal of Heat and Mass Transfer*, vol. 48, no. 8, pp. 1462–1469, 2005.

[2] Hu, X. J., Jain, A., and Goodson, K. E., Investigation of the Natural Convection Boundary Condition in Microfabricated Structures, *International Journal of Thermal Sciences*, vol. 47, no. 7, pp. 820–824, 2008.

[3] Bhowmik, H., and Tou, K. W., Experimental Study of Transient Natural Convection Heat Transfer From Simulated Electronic Chips, *Experimental Thermal and Fluid Science*, vol. 29, no. 4, pp. 485–492, 2005.

[4] Banerjee, S., Mukhopadhyay, A., Sen, S., and Ganguly, R., Natural Convection in a Bi-Heater Configuration of Passive Electronic Cooling, *International Journal of Thermal Sciences*, vol. 47, no. 11, pp. 1516–1527, 2008.

[5] Gad-El-Hak, M., *The MEMS Handbook*, CRC Press, Boca Raton, FL, 2001.

[6] Beskok, A., Karniadakis, G. E. and Trimmer, W., Rarefaction and Compressibility Effects in Gas Microflows, *Journal of Fluid Engineering*, vol. 118, no. 3, pp. 448–456, 1996.

[7] Karniadakis, G. E., and Beskok, A., *Microflows: Fundamentals and Simulation*, Springer-Verlag, New York, NY, 2002.

[8] Beskok, A., and Karniadakis, G. E., A Model for Flows in Channels, Pipes, and Ducts at Micro and Nano Scales, *Microscale Thermophysical Engineering*, vol. 3, no. 1, pp. 43–77, 1999.

[9] Chen, C. K., and Weng, H. C., Natural Convection in a Vertical Microchannel, *Journal of Heat Transfer*, vol.127, no. 9, pp. 1053–1056, 2005.

[10] Haddad, O. M., Abuzaid, M. M., and Al-Nimr, M. A., Developing Free-Convection Gas Flow in a Vertical Open-ended Microchannel Filled with Porous Media, *Numerical Heat Transfer Part A: Applications*, vol. 48, no. 7, pp. 693–710, 2005.

[11] Biswal, L., Som, S. K., and Chakraborty, S., Effects of Entrance Region Transport Processes on Free Convection Slip Flow in Vertical Microchannels With Isothermally Heated Walls, *International Journal of Heat and Mass Transfer*, vol. 50, no. 7–8, pp. 1248–1254, 2007.

[12] Chen, C. K., and Weng, H. C., Developing Natural Convection With Thermal Creep in a Vertical Microchannel, *Journal of Physics D: Applied Physics*, vol. 39, no. 14, pp. 3107–3118, 2006.

[13] Chakraborty, S., Som, S. K., and Rahul, A, Boundary Layer Analysis for Entrance Region Heat Transfer in Vertical Microchannels Within the Slip Flow Regime, *International Journal of Heat and Mass Transfer*, vol. 51, no. 11–12, pp. 3245–3250, 2008.

[14] Avci, M., and Aydin, O., Mixed Convection in a Vertical Parallel Plate Microchannel, *Journal of Heat Transfer*, vol. 129, no. 2, pp. 162–166, 2007.

[15] Avci, M., and Aydin, O., Mixed Convection in a Vertical Parallel Plate Microchannel with Asymmetric Wall

Heat Fluxes, *Journal of Heat Transfer*, vol. 129, no. 8, pp. 1091–1095, 2007.

[16] Weng, H. C., and Chen, C. K., Variable Physical Properties in Natural Convective Gas Microflow, *Journal of Heat Transfer*, vol. 130, no. 8, pp. 082401–8, 2008.

[17] Weng, H. C. and Chen, C. K., On the Importance of Thermal Creep in Natural Convective Gas Microflow With Wall Heat Fluxes, *Journal of Physics D: Applied Physics*, vol. 41, no. 11, pp. 1–10, 2008.

[18] Weng, H. C., and Chen, C. K., Drag Reduction and Heat Transfer Enhancement Over a Heated Wall of a Vertical Annular Microchannel, *International Journal of Heat and Mass Transfer*, vol. 52, no. 3–4, pp. 1075–1079, 2009.

[19] Buonomo, B., and Manca, O., Natural Convection Slip Flow in a Vertical Microchannel Heated at Uniform Heat Flux, *International Journal of Thermal Sciences*, vol. 49, no. 8, pp. 1333–1344, 2010.

[20] Kavehpour, H. P., Faghri, M., and Asako, Y., Effects of Compressibility and Rarefaction on Gaseous Flows in Microchannels, *Numerical Heat Transfer, Part A*, vol. 32, pp. 677–696, 1997.

[21] De-Yi, S., and Bu-Xuan, W., Effect of Variable Thermophysical Properties on Laminar Free Convection of Gas, *International Journal of Heat and Mass Transfer*, vol. 33, no. 7, pp. 1387–1395, 1990.

[22] Kennard, E. H., *Kinetic Theory of Gases*, McGraw-Hill, New York, NY, 1938.

[23] Suryanarayana, N. V., *Engineering Heat Transfer*, West Publishing Company, New York, NY, 1995.

[24] Weng, H. C., and Chen, C. K., A Challenge in Navier–Stokes-Based Continuum Modeling: Maxwell–Burnett Slip Law, *Phyics of Fluids*, vol. 20, pp. 106101-1-9, 2008.

[25] Lockerby, D. A., Reese, J. M., Emerson, D. R. and Barber, R. W., The Velocity Boundary Condition at Solid Walls in Rarefied Gas Simulations. *Physical Review E: Statistical Physics, Plasmas, Fluids, and Related Interdisciplinary Topics*, vol.70, no. 1, pp. 017303-1-4, 2004.

[26] Aung, W., Fully Developed Laminar Free Convection Between Vertical Plates, *International Journal of Heat and Mass Transfer*, vol. 15, pp. 1577–1580, 1972.

[27] Patankar, S. V., *Numerical Heat Transfer and Fluid Flow*, McGraw-Hill, New York, NY, 1980.

Behnam Rahimi is a Ph.D. student at the University of Victoria in Canada, working on the rarefied polyatomic gases. He obtained his bachelor's and master's degrees in applied sciences in 2008 and 2011, respectively, from Ferdowsi University of Mashhad in Iran. He also worked on gas flows and heat transfer in microscale devices at Microfluidics and Biomechanics Laboratory at Ferdowsi University of Mashhad.

Hamid Niazmand is a professor at Ferdowsi University of Mashhad in Iran. He received his Ph.D. in 1993 from the University of California Davis, USA. He has also performed collaborative research with University of Waterloo in Canada for more than 10 years. His main area of research is micro and nano flows. He also works in transport phenomena in cardiovascular systems and adsorption chillers.